Autonomously Controlled Homogenous Growth of Wafer-Sized High-Quality Graphene via a Smart Janus Substrate

Dongyun Wan, Tianquan Lin, Hui Bi, Fuqiang Huang, Xiaoming Xie, I.-Wei Chen, and Mianheng Jiang*

The work reports a new method for large-area growth of graphene films, which have been predicted to have novel and broad applications in the future. While chemical vapor deposition (CVD) is currently the preferred method, it suffers from a rather narrow processing window, and there is also much to be desired in the electrical properties of the CVD films. A new method for large-area growth of graphene films is reported to overcome the narrow processing window of the CVD method. A composite substrate made of a C-dissolving top (Ni) layer and a C-rejecting bottom (Cu) layer is designed, which evolves into a C-rejecting mixture, to autonomously regulate the C content at an elevated yet stable level at and near the surface over an extended duration. This "smart" substrate promotes graphene formation over a wide temperature-gas composition window, leading to reliable growth of wafer-sized graphene films of defined layer-thickness and superior electrical–optical properties. This "smart"-substrate strategy can also be implemented on Si and SiO_2 supports, paving the way toward the direct fabrication of large area, graphene-enabled electronic and photonic devices.

1. Introduction

Graphene has a unique two-dimensional hexagonal lattice structure and extraordinary physical properties.[1–3] Not surprisingly, large-area high-quality graphene films have been projected to enable many new applications. Atmosphere-pressure CVD (APCVD) is currently the preferred method for growing large-area graphene,[4–6] and CVD on Ni,[7] Cu[8] and Ru[9] substrates can provide large-area and transparent conducting graphene films, but their electrical properties are still less than desired and their processing conditions are severely restrictive. Previous work has emphasized the importance of catalysis and substrate surface structure on CVD.[7,8,10] Recently, the role of C solubility has been noted in non-CVD studies.[11,12] This is also relevant when CVD temperature is high enough to allow rapid C diffusion into the metal substrates, altering the level of C supersaturation at and near the surface, thus affecting the nucleation and growth kinetics of graphene.

Support for this argument is found in comparing two CVD metal substrates, Ni and Cu. Ni with a moderate C solubility of 0.4–2.7 at.% (Here at.% stands for the atomic percentage) over 700 °C–1300 °C yields a multilayer graphene film of small grains.[7,13–15] In contrast, Cu with little C solubility (<0.001 at.% at 1000 °C) yields a more uniform single-layered graphene film.[4,16] Unfortunately, the latter's stringent process conditions (temperature, pressure, gas composition, flow rate, etc.)[8,17] requiring a low C source content and a high temperature close to the melting point of Cu limits its utility for practical application. For example, while single-layered graphene is obtained on Cu at ~1000 °C under a low CH_4 concentration (<0.2%),[4,5] a higher CH_4 concentration results in an inhomogeneous film.[4]

One could argue that a C-insoluble substrate is conducive to uniform CVD growth, but the lack of a solid-state C source—provided by the C reservoir in the substrate and built up by C dissolution—to supplement the extraneous C source is the reason for the restrictive processing windows. This is because it would leave the C supply entirely to the surface reactions, which are extremely sensitive to the variations in gaseous and surface conditions. If so, one would call for an *ideal* substrate that embodies the design of being both C-soluble and C-insoluble, i.e., it is Janus-like but with only one reactive surface. We achieved this seemingly impossible feat by combining a C-dissolving top metal layer (e.g., Ni) and a C-rejecting base metal layer (e.g., Cu). Overtime, the two mutually miscible metals form an alloy (e.g., 0.9Cu:0.1Ni having a C solubility of 0.07 at.% at 1000 °C), which is also C-rejecting.[18] (That is, the two faces of Janus now merge into one!) We then envision the scenario depicted in **Figure 1**. At the start of CVD, the top layer can initially dissolve adsorbed C and serve as a C sink,

Dr. D. Y. Wan, Dr. T. Q. Lin, Dr. H. Bi, Prof. F. Q. Huang
CAS Key Laboratory of Materials for Energy Conversion
Shanghai Institute of Ceramics
Chinese Academy of Sciences
Shanghai 200050, P.R. China
E-mail: huangfq@mail.sic.ac.cn
Prof. X. M. Xie, Prof. M. H. Jiang
State Key Laboratory of Functional Materials for Informatics
Shanghai Institute of Microsystem and Information Technology
Chinese Academy of Sciences
Shanghai 200050, P.R. China
Prof. I.-W. Chen
Department of Materials Science and Engineering
University of Pennsylvania
Philadelphia, PA 19104, USA

DOI: 10.1002/adfm.201102560

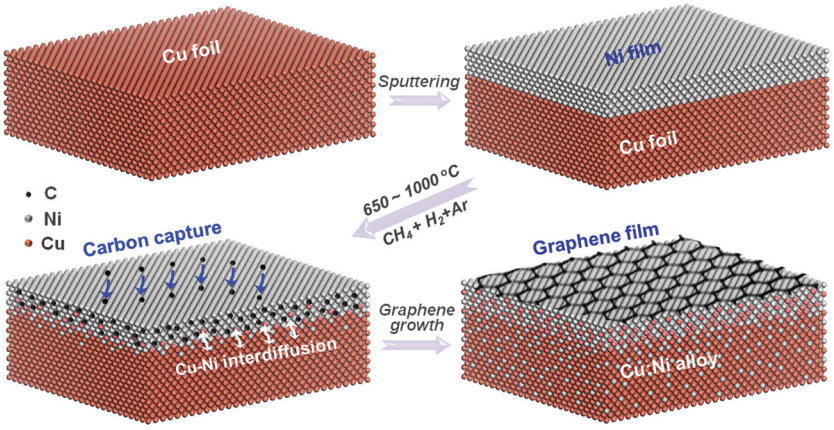

Figure 1. Schematic illustration of evolving "smart" bilayer substrate, on which graphene forms a uniform layer.

lessening the surface supersaturation of C and building up a pool of C supply. Next, after interdiffusion of the two metals, an alloy forms which acts as a C source, rejecting the stored C and supplying it to the surface. In this way, the self-evolving, "smart Janus" substrate can dynamically and autonomously regulate the C content at and near the surface, maintaining it at an elevated yet stable level for an extended time. This helps stabilize the nucleation and growth kinetics for graphene, thus lessening the sensitivity to the processing conditions.

2. Results and Discussion

We implemented the above mentioned "smart Janus" design using a Cu foil with a RF sputtered Ni film (e.g., 600 nm), referred to as Ni–Cu below. The substrate was treated in Ar-H_2 to remove surface oxide and to control grain size and surface quality, during which some Cu/Ni diffusion occurred so the top layer already contained some Cu. APCVD with CH_4 was next used to successfully grow single-layered graphene at above 950 °C and five-layered graphene at 650 °C, which is the lowest temperature ever reported for CH_4 APCVD. Further details of this method are provided in the Experimental Section, along with an example of the wafer-sized (Φ18 cm) graphene film (Figure S1 in Supporting Information) grown at 1000 °C under gas flow rates of Ar:H_2:CH_4 = 300:10:2 sccm. This CH_4 concentration of 0.64% is much higher than used in previous reports.[11,13]

Compared to the films grown on Cu shown in **Figure 2**d and Ni in Figure 2e under the same conditions, the above film on Ni–Cu (Figure S1, Figure 2a) is much more uniform with fewer wrinkles (an enlarged wrinkle can be seen in Figure 2b–c), flakes (only common in Figure 2d, on Cu) and grain boundaries (only common in Figure 2e, on Ni). Note that the film on Ni–Cu remains continuous on the steps (inherited from the substrate) and wrinkles, as shown in Figure 2b–c. These steps, which are also common on Ni and Cu surfaces[8,19,20] may have enabled step-flow growth,[21] which is deemed favorable for growing high-quality films. The SAED pattern in the inset of Figure 2a reveals that graphene on Ni–Cu is single-crystalline compared to that on Cu and Ni which is either a strained crystal (SAED in Figure 2d, on Cu) or a polycrystal (Figure 2e, on Ni). The film has a root-mean-square roughness of ~5 nm over an area spanning 300 nm according to Figure S2.

Raman spectra provided additional structural information of our films, as shown in Figure 2f. The film on Ni–Cu has a G band at 1584 cm^{-1} and a 2D band at 2695 cm^{-1}. The full-width half-maximum (FWHM) of the Lorentzian 2D band is ~30 cm^{-1}, and the intensity ratio I_{2D}/I_G is ~4; this indicates that it is a single-layered graphene.[22] In comparison, the film on Cu has a broader (FWHM ~45 cm^{-1}, centered at ~2700 cm^{-1}) and weaker 2D band (I_{2D}/I_G ~1) suggesting multiple layers, and the film on Ni which is of the lowest quality according to Figure 2e has an additional D band at 1350 cm^{-1}, which is commonly associated with defects.[22] To further evaluate the film uniformity, we randomly selected >100 locations in a wafer-sized film on Ni–Cu, and collected their Raman spectra. Single-layered graphene was found at more than 95% of these locations (Figure S3 in Supportining Information).

Growth on Ni–Cu has a relatively wide processing window. According to **Figure 3**a, wafer-sized graphene films grown at 1000 °C and 950 °C using a CH_4 flow rate from 2 to 20 sccm (Ar:H_2 = 300:10 sccm), corresponding to a CH_4 concentration from 0.64% to 6.1%, all exhibit single-layered graphene spectra. For comparison, high quality single-layered APCVD graphene only forms on Cu at CH_4 concentrations <0.2%.[4] Instead of CVD conditions, the Ni layer thickness is a robust control parameter. According to the I_{2D}/I_G and FWHM of the 2D band in Figure S4, the substrate with a 600 nm Ni layer yields the best single-layered film.

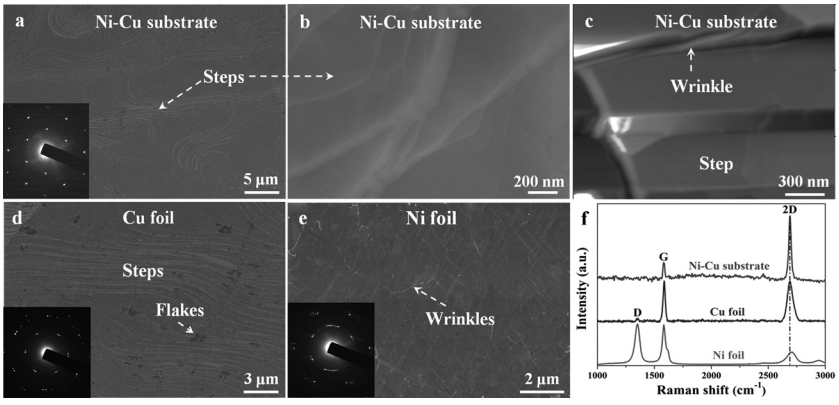

Figure 2. SEM images of graphene films on: a–b) Ni–Cu substrate, d) Cu foil, and e) Ni foil, with SAED patterns of the transferred films in the respective insets. c) AFM image of graphene on Ni–Cu substrate showing a step and a wrinkle. f) Raman spectra of the three graphene films. All films grown at 1000 °C under gas flow rates of Ar:H_2:CH_4 = 300:10:2 sccm.

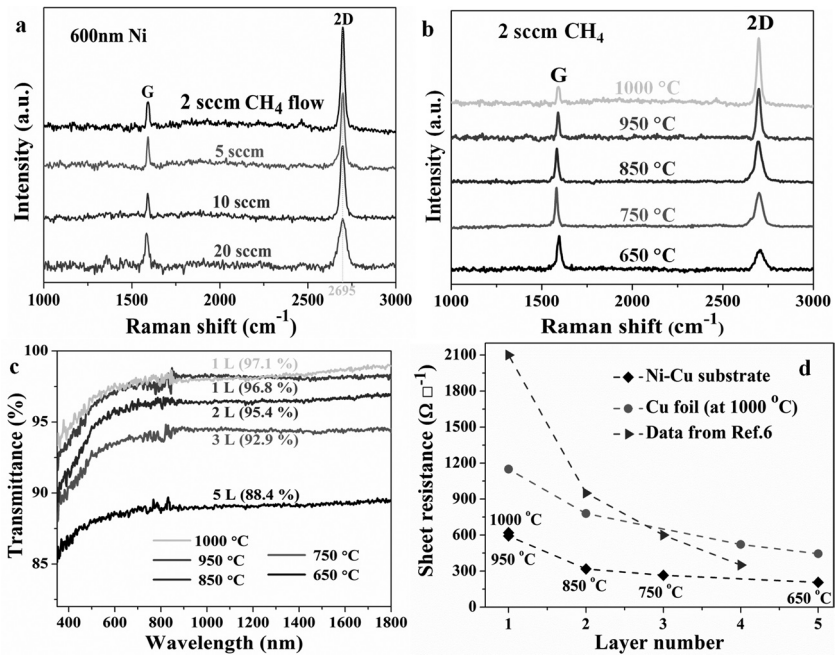

Figure 3. Raman spectra of graphene films grown on Ni–Cu substrates; a) at 1000 °C with different CH_4 flow rates, and b) at different temperatures. c) Optical transmittance and d) electrical sheet resistance of graphene films which have been removed from the metal substrate and transferred to a SiO_2 substrate. Some literature data[6] of resistance are included in (d) for comparison.

As the temperature is lowered, the film remains uniform over a large area as illustrated in Figure S5, albeit the number of layers increases. According to the I_{2D}/I_G ratio in Figure 3b, we obtained single-layered (1L) films at 1000 °C and 950 °C, double-layered (2L) films at 850 °C, three-layered (3L) films at 750 °C, and five-layered (5L) films at 650 °C, all at $Ar:H_2:CH_4$ = 300:10:2 sccm, and all highly uniform according to the microscopy images, Figure S5a–d. The folded film edges observed at high resolution are shown in the insets of Figure S5a–d to further illustrate their layer structure. Meanwhile, the absence of D band in their Raman spectra in Figure 3b confirms the high quality of the films. Therefore, homogenous multilayer graphene films can be grown even at 650 °C, which is the lowest growth temperature ever reported for APCVD.

The homogenity of the graphene films were examized by Raman mapping measurements on samples grown at 1000 °C (1L) and 850 °C (2L) on the smart substrates. Shown in **Figure 4** are the color-coded intensity mapping of G and 2D band intensity, and the corresponding 2D/G peak ratio mapping over an 80 × 60 μm² area. The upper set of the figure for 1000 °C, the lower set for 850 °C, and the color chart for the intensity to the right. The results clearly illustrate the uniform distribution of single-layer graphene over 95% of the area when grown at 1000 °C, and likewise of two-layer graphene when grown at 850 °C.

Optical and electrical properties in Figure 3c,d and **Table 1** were measured using graphene films removed from the metal substrate and transferred to a glass support. The optical transmittance (350–1800 nm) decreases from 100% by ~2.3% for each layer, so the transmittanceof the 1000 °C film shown in Figure 3c, 97.1% at 550 nm and over 98% in the near infrared region, indicates a single layer.[23] The 650 °C film has a transmittance of 87.4% at 550 nm, consistent with five layers. The electrical sheet resistance (R_{sq}) shown in Figure 3d also decreases with the layer thickness, as expected. Our 1L films have a sheet resistance of 620 Ω (grown at 1000 °C) and 593 Ω (grown at 950 °C), lower than that of a (2L) graphene film grown on Cu

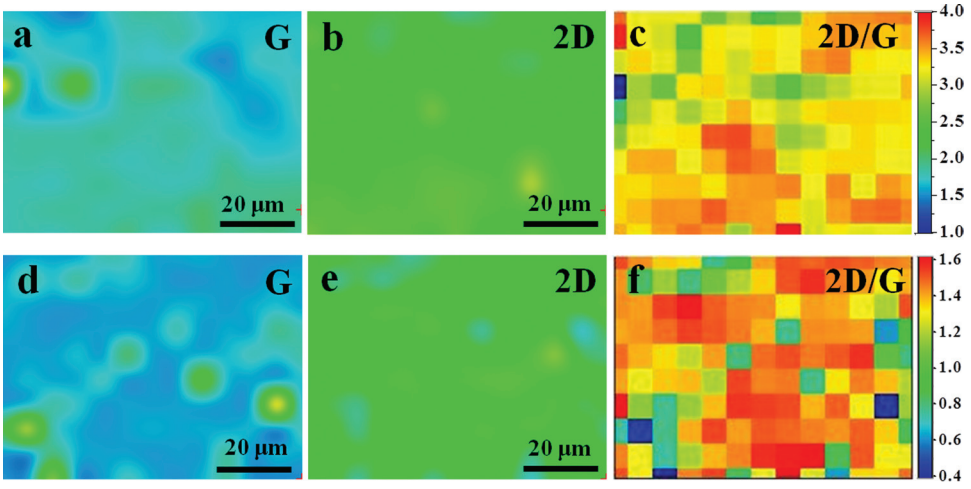

Figure 4. Raman mapping measurements of graphene films grown at 1000 °C (1L) and 850 °C (2L) on the smart substrates. Shown in the figures are the color-coded intensity mapping of G (a,d) and 2D band intensity (b,e), and the corresponding 2D/G peak ratio mapping (c,f) over an 80 μm × 60 μm area respectively. (The upper set for 1000 °C, the lower set for 850 °C, and the color chart for the intensity to the right.)

Table 1. Optical and electrical properties of graphene films of different layer thickness (No.) grown at different temperatures (T) on different substrates. Properties measured using films removed from the metal substrates and transferred to SiO_2 support. S-Cu used Cu foil, S-Ni used Ni foil, all others used Ni (600 nm)-Cu.

Sample	T [°C]	[Ni][a] [at.%]	Layer No.	Tr_{550}[b] [%]	R_{sq}[c] [Ω]	μ[d] [$cm^2\ V^{-1}\ s^{-1}$]
S-1000	1000	1.2	1	97.1	620	913.6
S-950	950	1.8	1	96.8	593	886.4
S-850	850	5.7	2	95.4	318	714.6
S-750	750	8.2	3	92.9	265	694.1
S-650	650	12.5	5	88.4	206	668.3
S-Cu	1000	0	2	95.5	1150	602.4
S-Ni[4]	1000	100	>5	83.7	>600	—

[a]Ni content of substrate after film growth, measured by energy-dispersive X-ray spectroscopy (EDX), taken at the surface with a penetration of ~1 mm; [b]Transmittance at 550 nm; [c]square resistance; [d]mobility.

at 1000 °C (1150 Ω). These values are better than the very best reported for single-layered APCVD graphene (typical values ranging from 700 to 1500 Ω).[24] This trend of superior electrical resistance compared to the literature data is held throughout the thickness range studied in Figure 3d. Note that even the 5L film grown at 650 °C has a 550 nm transmittance of 88.4% and an electrical square resistance of 206 Ω/sq, which are probably adequate for its use as a transparent conducting film. The mobility (μ in Table 1) measured by a four-probe method decreases as expected with increasing layer thickness, reaching 668.3 $cm^2\ V^{-1}\ s^{-1}$ in 5L films grown at 650 °C. The mobility of the 1L film grown at 1000 °C (913.6 $cm^2\ V^{-1}\ s^{-1}$) is superior to that grown on Cu at the same temperature (602.4 $cm^2\ V^{-1}\ s^{-1}$). These results are all supportive of the earlier claim of fewer defects in our films.

As mentioned previously, Cu has virtually no solubility for C whereas Ni has a considerable solubility—1.26 at.% at 1000 °C.[13] As shown in Table 1, after 1000 °C CVD, the surface (~1 μm) Ni content of the initially bilayered Ni–Cu is already low, meaning that it has been converted to a Cu:Ni alloy. (Some Cu/Ni diffusion already occurred in treated substrate prior to CVD.) This confirms our scenario (Figure 1) of metal interdiffusion that forms an alloy which tends to reject previously dissolved C. To study what film it provides when the alloy itself is used as a substrate, we prepared a Cu:Ni substrate by annealing a Ni (600 nm)-coated Cu foil at 1000 °C for 8 h, a condition that should allow an alloy to form. We then grew graphene on it at 1000 °C under 2 sccm CH_4 (i.e., 0.64%) as before. As shown in **Figure 5**a–c, the graphene grown is similar to the film grown on Cu foils (Figure 2d) at the same CH_4 (0.64%) concentration, predominantly discontinuous and multilayered. In Figure 5b,c, we also investigated graphene grown on a Ni (600 nm)-quartz substrate; it is similar to that grown on Ni foils (Figure 2e) having a defective multilayer graphene. This means that a Ni substrate of a thinner thickness (600 nm) behaves no differently from a thicker Ni foil. These experiments confirm that the synergetic combination of Ni and Cu, initially as distinct layers, is essential for the success of our Ni–Cu substrate, and the success cannot be duplicated by either a Cu:Ni alloy of the same final composition, or a Ni of the same top layer thickness but without a Cu backing.

We also apply the "smart" substrate to other supports commonly used for electronic and photonic applications; e.g., a bilayer of 600 nm Ni on top of 2 μm Cu sputtered onto a Si wafer, another onto a SiO_2 substrate. Under $Ar:H_2:CH_4$ = 300:10:2 sccm, we grew graphene on these supports at 1000–650 °C with very similar results, as shown in Figure 5d. The Raman spectra of the 1000 °C films, shown in Figure 5d, specifically the position (~2690 cm^{-1}) and FWHM (~35 cm^{-1}) of 2D band and the ratio of I_G/I_{2D} (~4), signal that these are 1L graphene of high quality and uniformity. Multilayer graphene was also obtained by decreasing the temperature to 650 °C, as shown in Figure 5d. The graphene films grown on these Ni–Cu coated semiconductor and dielectric substrates may be used for applications either directly or after a transfer, and our experience indicates that they are rather easy to remove and to transfer compared to the ones grown on commonly used metal substrates. (Direct growth at the dielectric interface beneath the metal may also be feasible.)[25]

To understand the origin of temperature and thickness dependence of graphene growth of both Ni and graphene, we next consider the interplay between C solubility and Cu/Ni interdiffusion in the substrate. Since C can take advantage of interstitial diffusion whereas Cu and Ni must rely on vacancy diffusion, C self diffusivity, D_C, is faster, with a lower activation

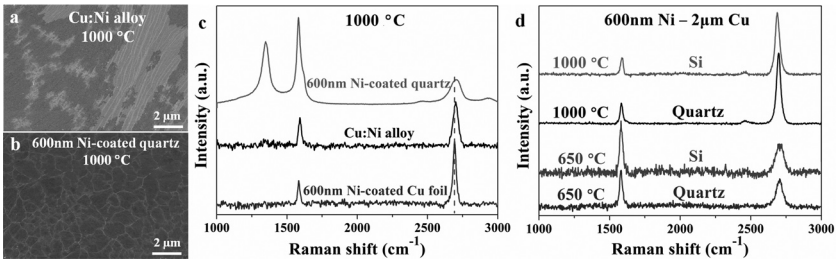

Figure 5. a–b) SEM images and c–d) Raman spectra of graphene samples on different substrates.

energy, Q_C, than Cu self diffusivity, D_{Cu}, (with Q_{Cu}) or its counterpart D_{Ni}. This conclusion should hold even when the dominant diffusion path gradually shifts from lattice at higher temperature to grain boundaries and dislocations at lower temperature.[13,26,27] Meanwhile, Cu melting 1085 °C is much more mobile than Ni melting at 1455 °C. Therefore, Cu/Ni alloying is dominated by D_{Cu}. In our experiments, two diffusion processes occur in the top layer of the substrate. i) Prior to and during CVD, Cu/Ni interdiffusion lowers the C solubility with a kinetics controlled by D_{Cu}. ii) During CVD, adsorbed C invades the substrate with a kinetics controlled by D_C. Therefore, the C incorporation and its spatial spread in the top layer are promoted by (i) but limited by (ii), meaning that they should scale with D_c/D_{Cu}.

The competition between (i) and (ii) is the basis for the self-regulating role of the "smart Janet" substrate, and it leads to several predictions. First, since $Q_{Cu} > Q_C$, D_C/D_{Cu} should increase with decreasing temperature. We thus predict the C concentration and spatial spread to increase at lower temperature. Assuming a higher C concentration is associated with a graphene film of more layers, it also predicts the graphene layer number to increase with decreasing temperature. This is already observed in Figure 3. Second, as long as the compositional evolution is still active, there should be a lessened sensitivity to processing conditions and to boundary conditions, e.g., temperature, gas composition and Ni-layer thickness. This explains the widening of processing window, which extends from 650 °C to 1050 °C and from 0.64% CH_4 to 6.1% CH_4. The limit of the processing window is determined by the unfavorable conditions when the substrate is no longer "smart" enough to cope: too thick a diffusion distance (i.e., the Ni layer thickness) or too low a temperature will bring about negligible compositional evolution, and conversely, too thin a diffusion distance or too high a temperature will exhaust the evolution before CVD ends or even during the prior heat-treatment. In our experiment, 600 nm is the optimal Ni thickness, but it can be varied by the treatment.

One compositional evidence in support of the above analysis is already found in Table 1, which shows that, at the end of CVD, the surface (within 1 μm) Ni content in the initially bi-layered Ni–Cu drops precipitously (to 1.2 at.% at 1000 °C) with the temperature. Further evidence comes from the compositional profiles (**Figure 6**) in the near surface region determined by X-ray photoelectron spectroscopy (XPS) aided by depth profiling. (More data in Tables S1 & S2.) The results include a Ni–Cu bilayer (Figure 6a), a Cu foil (Figure 6b), and a thoroughly pre-annealed Cu:Ni alloy same as in Figure 5a & 6c, which were all held at 1000 °C for 10 min under the same CVD condition. In addition, the Ni–Cu experiment was repeated at 650 °C (Figure 6d). These profiles are complicated by the artifacts, due to a large beam size and sputter-induced atom mixing during depth profiling, leaving misleading profiles suggesting C and O

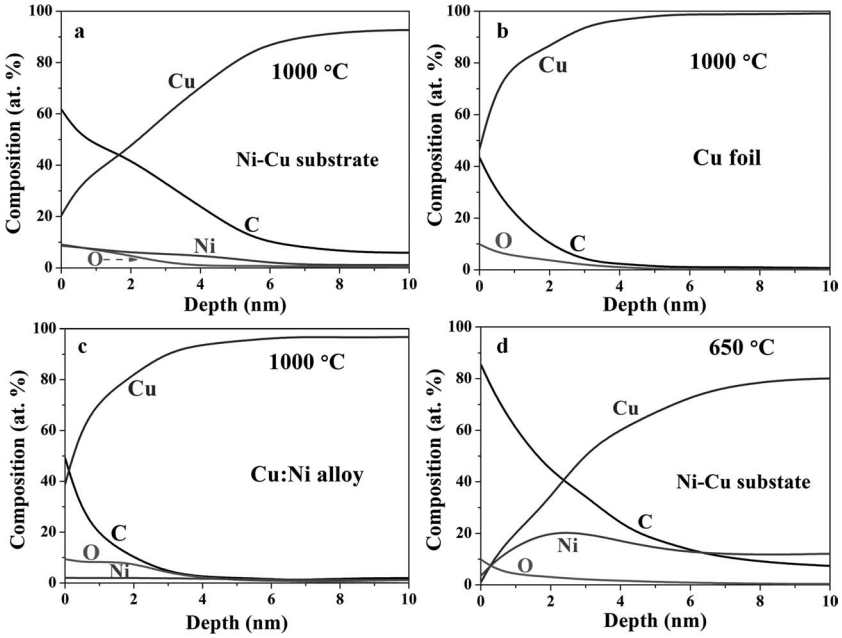

Figure 6. XPS depth profiles of a) 1000 °C Ni-coated Cu foil, b) 1000 °C Cu foil, c) 1000 °C Cu:Ni alloy previously annealed at 1000 °C for 8 hr, and d) 650 °C Ni-coated Cu foil, all held for 10 min under the same CVD flow ($Ar:H_2:CH_4$ = 300:10:2 sccm) condition at the respective temperature.

"in-diffusion" and Cu "out-diffusion" even in pure Cu with little C and O solubility (Figure 6b). But important insight can still be obtained after discounting the artifacts. First, Cu-Ni alloy (Figure 6c) behaves just like Cu (Figure 6b), so all its profiles are mere artifacts, and there is little real C and Cu diffusion. This is consistent with our observation of similar graphene growth on Cu-Ni alloy (Figure 5a) and on Cu (Figure 2d), neither of which is "smart" without the requisite compositional evolution. Second, there is much less Ni loss and Cu gain, but much more C in-diffusion (both in amount and spatial extent), at 650 °C (Figure 6d) than at 1000 °C (Figure 6a). Since there is relatively little Cu at the surface in these two samples, atom mixing by sputtering cannot generate the apparent Cu "diffusion" beneath the surface. So the Cu profiles in Figure 6a & 6d are real. This means that both substrates are "smart", as their compositions evolve in the way that follows the scenario in Figure 1. Indeed these profiles—Cu/Ni interdiffusion, the C content and spatial spread, as well as their temperature dependence—are in complete agreement with our predictions. The higher C content at the surface and in the near surface region at 650 °C is also consistent with the observation of 5L graphene.

The above mechanism involving counteracting thermodynamic (C solubility and Cu-Ni mixing) and kinetic (C and Cu/Ni diffusion) forces that drive the self-evolution of the "smart Janet" substrate to maintain an elevated C content and to control graphene synthesis is fundamentally different from previously proposed ideas for large-area graphene synthesis, such as the surface-catalysis or precipitation mechanism for CVD growth on Cu and Ni[7,8,10,19,28] and the segregation growth mechanism for non-CVD growth on Cu-Ni.[11,12] The "smart Janet" substrate makes CVD much more robust, having the processing temperature spanning over 350 °C, the CH_4 (carbon

source) pressure ranging over one order of magnitude, and the carbon layer number tunable from one to five. This in turn yields much better film quality (transmittance, resistance and mobility) over a coverage area that has no apparent size limit. As the concept of "smart" substrate along with the theoretical idea for autonomous control can also be adopted to other supports—metals, semiconductors, or dielectrics, it will hopefully help steer the future development of large scale fabrication of device-quality, defined layer-thickness graphene films for practical applications.

3. Conclusions

In summary, this work reports a new method for large-area growth of graphene films, which have been predicted to have novel and broad applications in the future. By using a new bilayered substrate for CVD method, the processing temperature now spans from 1000 °C to 650 °C, the CH_4 (carbon source) pressure can range over one order of magnitude, the carbon layer number can be tuned from one to five, the growth area has no apparent size limitation (we report wafer-sized ones), and the combined optical, electrical properties (transmittance, resistance and mobility) far exceed the best previously reported for large-area graphenes. Moreover, this new substrate design has been adopted to grow graphene on silicon and SiO_2 to enable future electronic and photonic applications. The concept of smart substrate along with its theoretical underpinning will have a huge impact on the future development of large scale fabrication of device-quality, defined layer-thickness graphene films for practical applications.

4. Experimental Section

Deposition of Ni-coated Cu Films: To form the smart substrate, a Ni layer was deposited on a Cu foil (Alfa Aesar) in a JPG450 magnetron sputtering system equipped with a 3 in. magnetron gun (US'GUN). The RF power (13.56 MHz) was supplied by an RF generator (Advanced Energy) matched to the target by a tuning network (Advanced Energy). A Ni target (99.99% purity) was used. An unthrottled base pressure of 2.0×10^{-4} Pa was reached using a combined vacuum system of mechanical pumping and turbomolecular pumping. All the experiments were conducted under a flow of high-purity Ar gas (99.99%) at 10 sccm, typically with the working pressure of 1.0 Pa at a sputtering power of 120 W. The maximum temperature monitored on the unheated substrate during sputtering is 55 °C.

Graphene Growth: The Ni-coated copper foils were placed in a quartz tube furnace and heated to 650–1000 °C in the presence of a mixture of hydrogen and argon. The substrate was first annealed for 10 min to coarsen Ni and Cu grain size, to remove residual nickel oxide and to smooth the surface. Subsequently, methane gas was introduced to the furnace and the CVD synthesis was performed for 10 min. The H_2 and Ar flow rate during CVD was 10:300 sccm in all cases and the CH_4 flow rate was varied from 2 to 20 sccm. Uniform graphene deposition was achieved independent of the size of the substrate, indicating no size limitation other than the physical constraint of the furnace.

Transferring Graphene to Target Substrates: CVD graphene films grown on Ni–Cu was transferred to the target substrate using a developed effective method. A ~300 nm thick Au film was first deposited on one side of the Cu:Ni alloy substrate, then PMMA was spin coated on the other side of the substrate. The sandwich structure (Au/graphene/Ni–Cu/graphene/PMMA) was placed into a 0.2 mol L^{-1} $FeCl_3$ solution to etch away the Ni–Cu substrate, and the remaining graphene/PMMA was placed into deinoized water. Finally, after the removal of the PMMA film in hot acetone, the graphene domains were transferred onto target substrates or Cu grids for measurements.

Characterizations: A Hitachi S-4800 FESEM operating at 1 kV was used to investigate the morphologies. Raman spectra were collected on a thermal dispersive spectrometer using a laser with an excitation wavelength of 532 nm at laser power of 10 mW. TEM were conducted using a JEOL 2100F microscope, operating at 200 kV. Graphene grown on Ni-coated Cu foils was transferred to a TEM grid (Quantifoil Cu 200 mesh) for these investigations. AFM images of topography were recorded using a Seiko SPI 3800 N probe station. XPS experiments were carried out on a RBD upgraded PHI-5000C ESCA system (Perkin Elmer) with Mg Kα radiation (hν = 1253.6 eV). The optical properties of wafer-sized graphene films were measured by a Hitachi U4100 UV–vis-NIR spectrometer. The sheet resistances and electron mobility of wafer-sized graphene films were measured by the four-probe Van Der Pauw method with an Accent HL5500.

Supporting Information

Supporting Information is available from the Wiley Online Library or from the author.

Acknowledgements

D.W. and T.L. contributed equally to this work. The authors thank Prof. Jing Sun for the instrumental help. Financial supports from National 973 & 863 Program of China Grant Nos. 2009CB939903 & 2011AA050505, National Science and Technology Major Project Grant No. 2011ZX02707, NSF of China Grant Nos. 51102263, 91122034, 51125006, 50821004, & 21101164, NSF of Shanghai Grant No.11ZR1441900, and Science and Technology Commission of Shanghai Grant Nos. 10520706700 & 10JC1415800. I.W.C. was supported by the US NSF Grant No. DMR-1104530, primarily, and DMR-0907523 and DMR-1120901, in part.

Received: October 24, 2011
Revised: November 28, 2011
Published online: January 9, 2012

[1] K. S. Novoselov, A. K. Geim, S. V. Morozov, D. Jiang, Y. Zhang, S. V. Dubonos, I. V. Grigorieva, A. A. Firsov, *Science* **2004**, *306*, 666.
[2] A. K. Geim, K. S. Novoselov, *Nat. Mater.* **2007**, *6*, 183.
[3] A. K. Geim, *Science* **2009**, *324*, 1530.
[4] S. Bhaviripudi, X. Jia, M. S. Dresselhaus, J. Kong, *Nano Lett.* **2010**, *10*, 4128.
[5] H. Bi, F. Huang, J. Liang, X. Xie, M. Jiang, *Adv. Mater.* **2011**, *23*, 3202.
[6] X. Li, Y. Zhu, W. Cai, M. Borysiak, B. Han, D. Chen, R. D. Piner, L. Colombo, R. S. Ruoff, *Nano Lett.* **2009**, *9*, 4359.
[7] K. S. Kim, Y. Zhao, H. Jang, S. Y. Lee, J. M. Kim, K. S. Kim, J. H. Ahn, P. Kim, J. Y. Choi, B. H. Hong, *Nature* **2009**, *457*, 706.
[8] X. Li, W. Cai, J. An, S. Kim, J. Nah, D. Yang, R. Piner, A. Velamakanni, I. Jung, E. Tutuc, S. K. Banerjee, L. Colombo, R. S. Ruoff, *Science* **2009**, *324*, 1312.
[9] S. Marchini, S. Günther, J. Wintterlin, *Phys. Rev. B* **2007**, *76*, 075429.
[10] X. Li, W. Cai, L. Colombo, R. S. Ruoff, *Nano Lett.* **2009**, *9*, 4268.
[11] N. Liu, L. Fu, B. Dai, K. Yan, X. Liu, R. Zhao, Y. Zhang, Z. Liu, *Nano Lett.* **2010**, *11*, 297.
[12] X. Liu, L. Fu, N. Liu, T. Gao, Y. Zhang, L. Liao, Z. Liu, *J. Phys. Chem. C* **2011**, *115*, 11976.
[13] J. J. Lander, H. E. Kern, A. L. Beach, *J. Appl. Phys.* **1952**, *23*, 1305.

[14] M. Eizenberg, J. M. Blakely, *Surf. Sci.* **1979**, *82*, 228.
[15] J. C. Shelton, H. R. Patil, J. M. Blakely, *Surf. Sci.* **1974**, *43*, 493.
[16] G. A. López, E. J. Mittemeijer, *Scripta Mater.* **2004**, *51*, 1.
[17] S. Bae, H. Kim, Y. Lee, X. Xu, J. S. Park, Y. Zheng, J. Balakrishnan, T. Lei, H. Kim, Y. I. Song, Y. J. Kim, K. S. Kim, B. Ozyilmaz, J. H. Ahn, B. H. Hong, S. Iijima, *Nat. Nanotech.* **2010**, *5*, 574.
[18] M. E. Nicholson, *Trans. Metall. Soc. AIME* **1962**, *224*, 533.
[19] S. J. Chae, F. Güneş, K. K. Kim, E. S. Kim, G. H. Han, S. M. Kim, H. J. Shin, S. M. Yoon, J. Y. Choi, M. H. Park, C. W. Yang, D. Pribat, Y. H. Lee, *Adv. Mater.* **2009**, *21*, 2328.
[20] D. Usachov, A. M. Dobrotvorskii, A. Varykhalov, O. Rader, W. Gudat, A. M. Shikin, V. K. Adamchuk, *Phys. Rev. B* **2008**, *78*, 085403.
[21] P. W. Sutter, J. I. Flege, E. A. Sutter, *Nat. Mater.* **2008**, *7*, 406.
[22] A. C. Ferrari, J. C. Meyer, V. Scardaci, C. Casiraghi, M. Lazzeri, F. Mauri, S. Piscanec, D. Jiang, K. S. Novoselov, S. Roth, A. K. Geim, *Phys. Rev. Lett.* **2006**, *97*, 187401.
[23] R. R. Nair, P. Blake, A. N. Grigorenko, K. S. Novoselov, T. J. Booth, T. Stauber, N. M. R. Peres, A. K. Geim, *Science* **2008**, *320*, 1308.
[24] Z. Sun, Z. Yan, J. Yao, E. Beitler, Y. Zhu, J. M. Tour, *Nature* **2010**, *468*, 549.
[25] C. Y. Su, A. Y. Lu, C. Y. Wu, Y. T. Li, K. K. Liu, W. Zhang, S. Y. Lin, Z. Y. Juang, Y. Zhong, F. R. Chen, L. J. Li, *Nano Lett.* **2011**, *11*, 3612.
[26] B. S. Berry, *J. Appl. Phys.* **1973**, *44*, 3792.
[27] G. O. Trønsdal, H. Sørum, *Phys. Status Solidi B* **1964**, *4*, 493.
[28] X. Li, C. W. Magnuson, A. Venugopal, J. An, J. W. Suk, B. Han, M. Borysiak, W. Cai, A. Velamakanni, Y. Zhu, L. Fu, E. M. Vogel, E. Voelkl, L. Colombo, R. S. Ruoff, *Nano Lett.* **2010**, *10*, 4328.